ADVANCED FUNCTIONAL MATERIALS

www.afm-journal.de

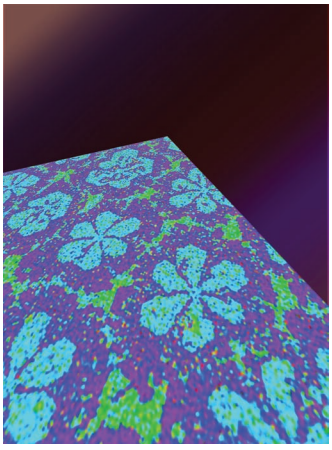

Thermomagnetic Materials

On page 1822, Benjamin Balke and co-workers report the thermodynamically stable phase separation of a Heusler compound induced by rapid cooling from the liquid phase. A linear combination of the different element-specific energy-dispersive X-ray (EDX) mappings (with brightness proportional to the concentration) is shown. The phase separation forms an ordered 3D flower-like structure on the microscale.

Quantum Dots

On page 1843, Dong Soo Lee, Yoon-Sik Lee, and co-workers investigate very bright quantum dot (QD)-based probes for effective bioimaging. Silica-coated, QD-embedded silica nanoparticles (Si@QDs@Si NPs) containing QDs composed of CdSe@ZnS (core-shell) are prepared to compare the structure-based advantages with single QDs having similar quantum yields. The excellence of Si@QDs@Si NPs is illustrated by significantly enhanced fluorescence signals. The more advanced version of QDs-based silica nanoparticles containing multishell QDs is prepared without significant loss of quantum yield during surface modification.

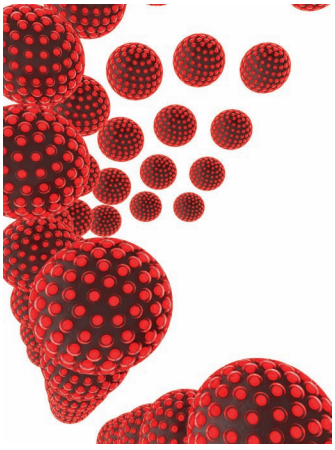

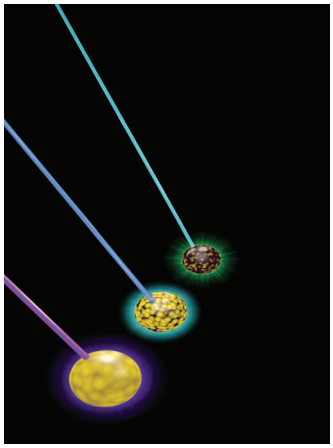

Gold Nanoparticles

The image shows three gold nanoparticles with varying levels of surface adsorbate (shown as brown patches on nanoparticle surface) but that are otherwise identical. Both the excitation and emission spectra shift as a result; this is indicated by varying colors of exciting laser beams and simultaneously varying colors of nanoparticle fluorescence. The article by Ewa M. Goldys and Mushtaq A. Sobhan on page 1906 explains the microscopic mechanism behind this observation.

CONTENTS

FEATURE ARTICLE

Semiconductors

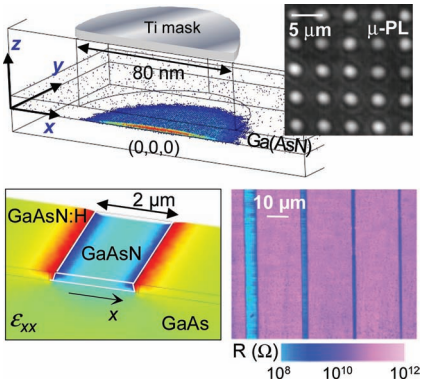

The remarkable consequences of hydrogen irradiation on the electronic, structural, optical, and electrical properties of GaAsN are exploited to specifically create artificial heterostructures for different applications. The highly trapping-limited diffusion of H atoms in dilute nitrides allows for the modulation of the material properties in the growth plane, thus allowing for fabrication of site-controlled quantum dots, engineering of the strain field, and patterning of the electrical resistance.

FULL PAPERS

Magnetic Materials

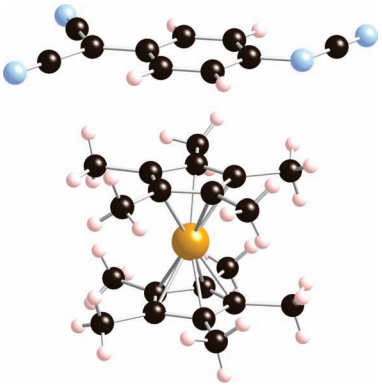

A new family of organic magnets with N,7,7-tricyanoquinomethanimine (TCQMI) is reported. $[Fe^{III}(C_5Me_5)_2]^{\bullet+}[TCQMI]^{\bullet-}$ forms parallel chains of alternating radical cations/anions and orders at 3.4 K as a weak ferromagnet. Amorphous $M[TCQMI]_2 \bullet z\ CH_2Cl_2$ (M = V, Fe) have μ_4-$[TCQMI]^{\bullet-}$, and the Fe compound is a weak ferromagnet at ≈4 K, whereas the V compound does not magnetically order.

Self-Assembly

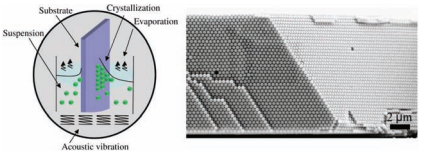

A tenfold improvement of the in-plane lattice ordering in opal films is achieved using the non-equilibrium self-assembly of colloidal suspension under agitation by noise vibrations. A new and robust quantitative method of surface lattice ordering characterization is applied and results are compared with the optical diffraction at high-index crystal planes.

Thermomagnetic Materials

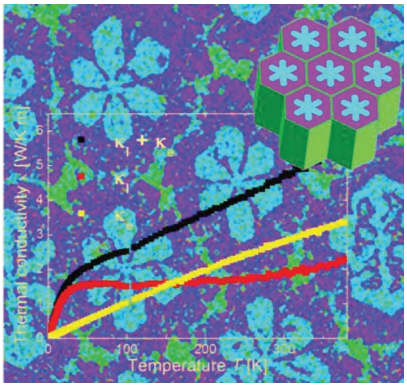

A thermodynamically stable phase separation of $Co_2Dy_{0.5}Mn_{0.5}Sn$ into the Heusler compound Co_2MnSn and $Co_8Dy_3Sn_4$ is induced by rapid cooling from the liquid phase. The phase separation forms an ordered flower-like structure on the microscale. The increased scattering of phonons at the phase boundaries reduces the thermal conductivity and thus improves thermoelectric and spin-caloric properties.

FULL PAPERS

Reversible bistable current with a switching effect of the electron field emission from surface transfer doped ultra-nanocrystalline diamond thin films is reported. This switching is manifested by abrupt jumps in the current emission at specific extracting electric field values. Persistent hysteresis is exhibited whenever the field is ramped down. This finding may lead the way to novel memory switch devices with unprecedented performance.

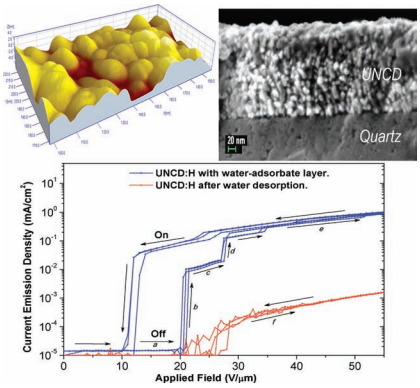

Nanostructures

Efficient local gene transfection on a tissue scaffold is of crucial importance in facilitating tissue repair and regeneration. The gelatin-functionalized polycaprolactone (PCL) film surfaces are prepared via surface-initiated atom transfer radical polymerization (ATRP) of glycidyl methacrylate (GMA), which could enhance the cell-adhesion and local gene transfection properties. With the pre- and post-loading sandwich-like gene transfection, the gelatin-functionalized PCL film surface can substantially enhance the transfection properties to different cell lines.

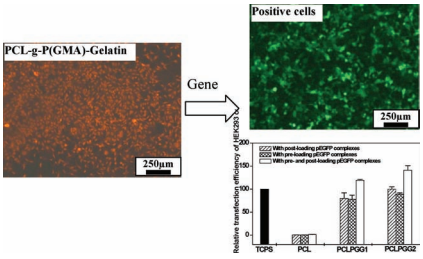

Tissue Engineering

Very bright quantum dot (QD)-based probes consisting of QDs on 120 nm silica nanoparticles with silica shells are investigated for effective bioimaging. Silica-coated, QD-embedded silica nanoparticles exhibit approximately 200-times stronger photoluminescence (PL) than single QDs. The more advanced version of QD-based silica nanoparticles containing multishell QDs can detect as few as 400 units of nanoparticle-internalized cells in a cell-implanted mouse model.

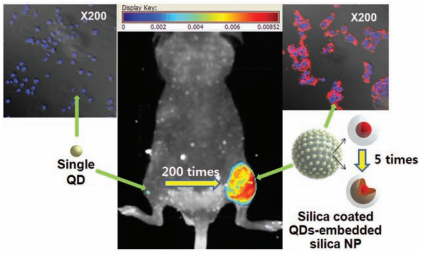

Quantum Dots

Ferromagnetic Fe_3P films are readily deposited on quartz substrates at 400 °C using the single-source molecular precursors $H_2Fe_3(CO)_9PR$ (R = ^{t}Bu or Ph) in a simple, low-pressure metal-organic chemical vapor deposition (MOCVD) apparatus. The films exhibit exceptional phase purity and the structural, spectroscopic, and magnetic data obtained from the films agree well with data obtained from pure bulk Fe_3P.

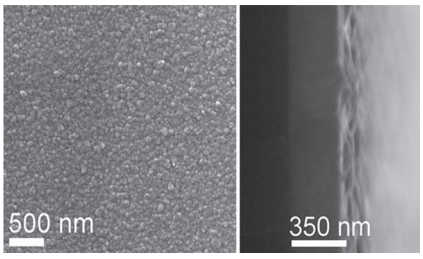

Magnetic Materials

CONTENTS

FULL PAPERS

Self-Assembly

The growth orientation of semiconductor molecules at a gold/self-assembled monolayer (SAM)/semiconductor interface preserves the molecular long axis orientation along the substrate normal, in contrast to a bare gold/semiconductor interface. As a result, the film microstructure is well-organized for charge transport in the interfacial region.

Biomaterials

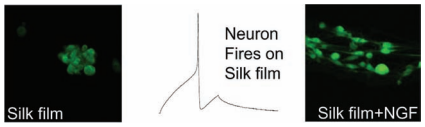

Silk fibroin (SF) is a natural biomaterial with huge potential for use as a biofunctional interface in electronic devices that aim to stimulate and control neural network activity and peripheral nerve repair. SF films support the adherence and growth of peripheral sensory neurons, preserve neuronal functionalities, and can be funtionalized with trophic factors to promote neurite outgrowth.

Luminescence

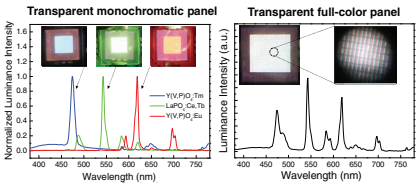

Using hydrothermally synthesized red $Y(V_{0.5},P_{0.5})O_4$:Eu, blue $Y(V_{0.5},P_{0.5})O_4$:Tm, and green $LaPO_4$:Ce,Tb nanophosphors highly transparent emissive layers are screen-printed. Monochromatic test panels of transparent plasma display are fabricated by the simple combination of the rear plate (nanophosphor/glass) with the front plate of the current ac-plasma display panels and a white luminescent full-color transparent panel is demonstrated.

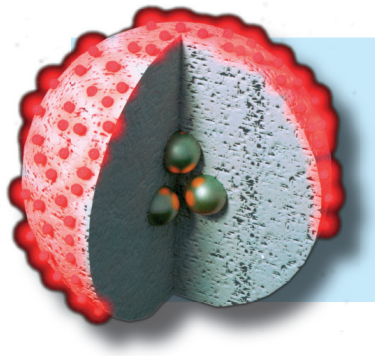

How to contact us:

Editorial Office:
Phone: (+49) 6201-606-235/531
Fax: (+49) 6201-606-500
Email: afm@wiley-vch.de

Reprints:
cherth@wiley-vch.de

Copyright Permission:
Fax: (+49) 6201-606-332
Email: rights@wiley-vch.de

FULL PAPERS

Preparation, isolation, and rapid unambiguous characterization of large size ultrathin layers of MoS_2, GaS, and GaSe onto SiO_2/Si substrates is reported. The optical contrast of these thin layers is correlated with atomic force microscopy (AFM), Raman spectroscopy, and Raman imaging to determine the exact thickness and to calculate number of atomic layers present in the thin flakes/sheets in a fast, non-destructive, and unambiguous manner.

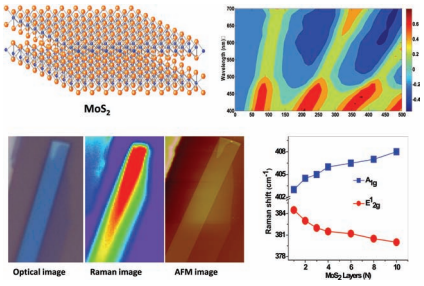

Layered Materials

Rapid Characterization of Ultrathin Layers of Chalcogenides on SiO_2/Si Substrates

The fluorescence emission/excitation energies of gold nanoparticles of various types are shown to follow variations in the electrostatic potential at their surface. The fluorescence shifts, the evolution of zeta potentials, and the fluorescence intensity trends are explained by a model of the principal fluorescence transitions that takes into account the nanoparticle surface ligands.

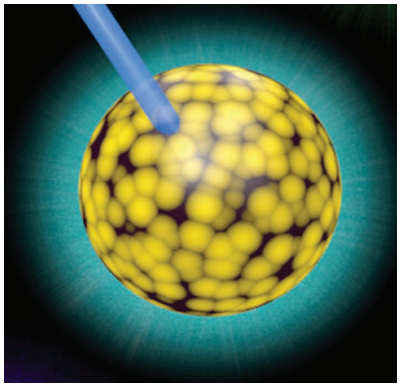

Gold Nanoparticles

Fluorescence of Colloidal Gold Nanoparticles is Controlled by the Surface Adsorbate

Monodisperse microparticles with adjustable diameter composed from pure protein (insulin or catalase) are prepared under gentle conditions by hard-templating on porous decomposable $CaCO_3$ microtemplates via isoelectric precipitation followed by pH- or EDTA-mediated template removal. The mechanism of the particle formation, mechanical properties, protein release, and potential for drug delivery applications are addressed.

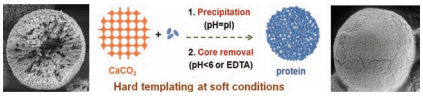

Drug Delivery

One-Step Formulation of Protein Microparticles with Tailored Properties: Hard Templating at Soft Conditions

Large, dense shapes of nanoblended polyelectrolyte complex are produced for the first time. Properties and processing are influenced by the salt concentration of solutions to which the complexes are exposed. A macroscopic tube, of dimensions similar to blood vessels, is an example of the new morphologies accessible.

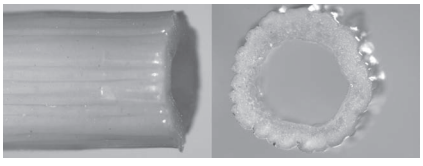

Composite Materials

Extruded Saloplastic Polyelectrolyte Complexes

CONTENTS

FULL PAPERS

Self-Assembly

Stimuli-Free Reversible and Controllable Loading and Release of Proteins under Physiological Conditions by Exponentially Growing Nanoporous Multilayered Structure

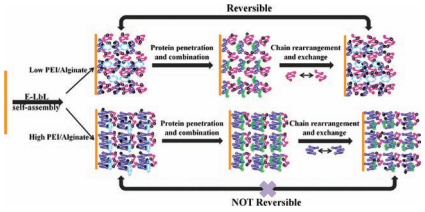

A novel nanoporous multilayered poly(ethyleneimine)(PEI)/alginate film is fabricated by exponentially growing, layer-by-layer self-assembly to serve as a carrier for protein loading and release. It is demonstrated to be the first artificial system reported with the capability of stimuli-free reversible loading and release of proteins under physiological conditions and thus has great potential for various biomedical applications.

Magnetic Nanoparticles

Self-Assembled Complexes of Horseradish Peroxidase with Magnetic Nanoparticles Showing Enhanced Peroxidase Activity

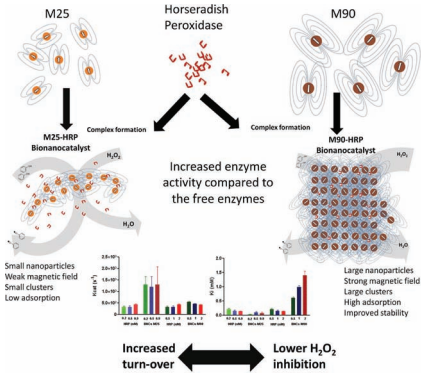

Self-assembled bio-nanocatalysts (BNCs) of magnetite and horseradish peroxidase demonstrate novel catalytic properties depending on the magnetic nanoparticles used (size, magnetism, surface area). The new properties can be attributed to magnetic field effects at the nanoscale and the mesoporous properties of the assemblies on the reaction schemes of enzymes. BNCs offer new opportunities to expand the use of peroxidase-related enzymes for industrial bioprocesses.

Microporous Materials

The Performance of Small-Pore Microporous Aluminophosphates in Low-Temperature Solar Energy Storage: The Structure–Property Relationship

A model that predicts the heat storage potential of numerous known or new microporous aluminophosphates is proposed based on a comparative thermogravimetric and calorimetric study of three known structures. The formation of highly ordered water clusters in the pores is determined to be a driving force for sudden water uptake in a narrow relative pressure range.

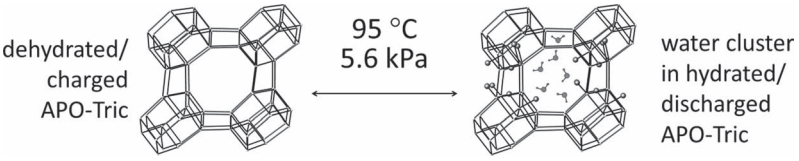

Fuel Cells

Understanding Chemical Expansion in Non-Stoichiometric Oxides: Ceria and Zirconia Case Studies

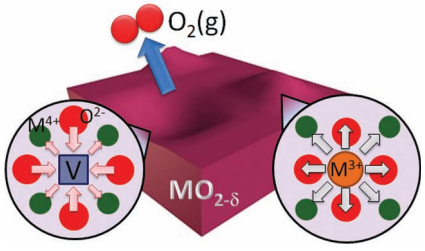

Formation of an oxygen vacancy (leading to a lattice contraction) with simultaneous cation radius increase (leading to a lattice expansion), which is investigated by atomic scale computational and empirical modeling, results in a chemical expansion of a non-stoichiometric oxide. Material compositions with minimal coefficient of chemical expansion, avoiding mechanical instabilities in high temperature applications, are predicted.

FULL PAPERS

Monodisperse mesoporous zirconium titanium oxide microspheres with varying compositions, high surface areas, and well-interconnected mesopores are successfully synthesized via a combined sol–gel self-assembly and solvothermal process. The resulting microspheres show potential for heavy metal ion sequestration from aqueous solution.

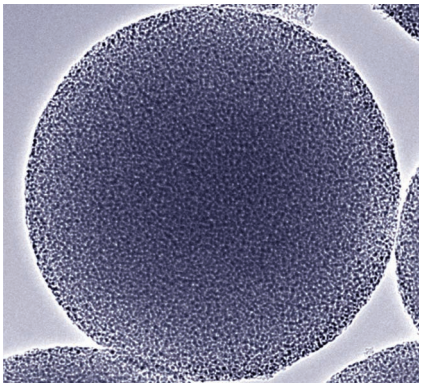

Self-Assembly

Nanolaminates with alternating layers of $Cu_{50}Zr_{50}$ metallic glasses (MG) and polyisoprene are synthesized and nanolaminate-containing nanopillars are fabricated. Compared with monolithic metallic glasses and MG-metal nanolaminates, these novel materials exhibit >30% enhancement in deformability without sacrifice in strength, with a concurrent suppressed stochastic signature.

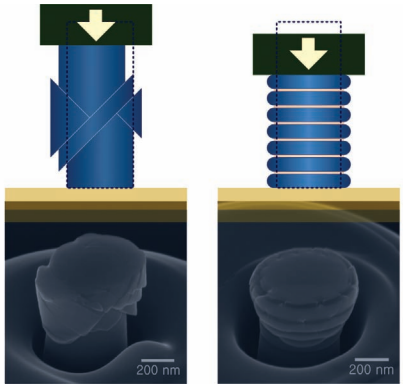

Glass

A facile and mild strategy to synthesize K-modified graphene using the room-temperature chemical modification of K in the graphene is demonstrated. The as-prepared K-modified graphene, used as an advanced electrode material, exhibits excellent electrocatalytic activity toward the oxidation of NO_2^- and is successfully applied in the determination of NO_2^- in vitro and from cancer cells.

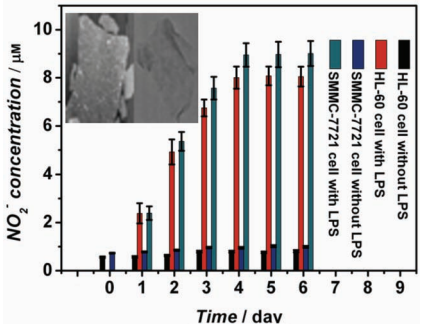

Graphene